Retro Diels−Alder Reactions of 5,6-Disubstituted-7-oxabicyclo[2.2.1]hept-2-enes: Experimental and Density Functional Theory Studies

Jason T. Manka,[†] Andrew G. Douglass,[†,‡] Piotr Kaszynski,[‡] and Andrienne C. Friedli*[,†,‡]

Department of Chemistry, Middle Tennessee State University, Murfreesboro, Tennessee 37132

afriedli@mtsu.edu

Several 5,6-disubstituted-7-oxabicyclo[2.2.1]hept-2-enes (**1**−**4**) were synthesized on ≥0.1 mol scale. The heat-induced retro Diels−Alder (rDA) decomposition of these derivatives was studied by thermal analysis, and the kinetics of the rDA were measured for **4**. First-order rate constants ($k = 1.91$− 14.2×10^{-5} s^{-1}), measured at four temperatures between 124 and 150 °C, were used to calculate Arrhenius activation parameters E_a (34.5 ± 0.5 kcal/mol) and ln A (1.77 ± 0.03 × 10^4). The observed activation energy was significantly larger (by 9.5 kcal/mol) than that previously measured for the maleic anhydride adduct **1**, and this was attributed to the difference in LUMO energies for the two dienophiles. Modeling of the activation parameters found for **4** with density functional theory (DFT) calculations for similar compounds **5** and **6** gave close quantitative correlations for $\Delta H^\ddagger$, $\Delta G^\ddagger$, $\Delta S^\ddagger$. The rDA reactions studied were found to be entropy-driven.

Introduction

The classical Diels−Alder (DA) adduct 7-oxabicyclo-[2.2.1]hept-5-ene-2,3-dicarboxylic anhydride (**1**) is a key starting material for a variety of biologically relevant compounds[1] and polymers.[2−5] Among the polymers are polyelectrolytes, which we have pursued[6,7] for applications in solid-state batteries. Polyethers are particularly well-suited for ion conduction[8] and can be synthesized from diol **2**, monoether **3**, and diether **4** via **1**.

One important issue in the preparation of polymers is the purity of the monomers. This is a concern in the case of monomers **1**−**4**, which can undergo retro Diels−Alder (rDA) reactions upon heating. The rDA decomposition of **1** does not pose a serious obstacle to its synthesis. However, the limited thermal stability of **1**−**4** does intefere with purification, since for large scale preparations of these products, recrystallization (for **1**) or vacuum distillation (for **2**−**4**) is preferable to chromatography.

Although the syntheses of **2**−**4** have been described in the literature on various scales,[3,4,9] there are no experi-

mental or theroretical investigations of their thermal stability aside from our initial observations.[7] In fact, there are very few experimental[1,10] and theoretical[11] studies of DA adducts of furan aside from **1**. Compound **1** is the most extensively characterized derivative of 7-oxabicyclo[2.2.1]hept-2-ene, with X-ray structural data[12] and theoretical[13] as well as kinetic and thermodynamic studies at atmospheric[14,15] and elevated[16,17] pressures reported.

Therefore, we were interested in gaining a detailed understanding of the kinetics and thermodynamics of the rDA for **2**−**4** and comparing the results to those for **1**. Here we describe the convenient large scale preparation and isolation of compounds **2**−**4** and the kinetics of the rDA reaction for a representative compound, **4**. The experimental results are compared with those for **1** and discussed in the context of DFT calculations for **1** and model compounds **5** and **6**.

Results and Discussion

Synthesis. Syntheses of **2**−**4** were carried out according to Scheme 1. The classical Diels−Alder reaction of furan (**7**) and maleic anhydride (**8**) resulted in a mixture of crystalline **1-exo** contaminated with **1-endo** in amounts determined by reaction time.[18] Without purification, the

* Author for correspondence: Phone/fax: 615-898-2071/5182.
† Department of Chemistry, Middle Tennessee State University, Murfreesboro, TN 37132.
‡ Department of Chemistry, Vanderbilt University, Nashville, TN 37235.

(1) Vogel, P.; Cossy, J.; Plumet, J.; Arjona, O. *Tetrahedron* **1999**, *55*, 13521−13642.
(2) Lu, S.-Y.; Quayle, P.; Heatley, F.; Booth, C.; Yeates, S. G.; Padget, J. C. *Macromolecules* **1992**, *25*, 2692−2697.
(3) Lu, S.-Y.; Armass, J. M.; Majid, N.; Glennon, D.; Byerley, A.; Heatley, F.; Quayle, P.; Booth, C.; Yeates, S. G.; Padget, J. C. *Macromol. Chem. Phys.* **1994**, *195*, 1273−1288.
(4) Novak, B. M.; Grubbs, R. H. *J. Am. Chem. Soc.* **1988**, *110*, 960−961.
(5) Manning, D. D.; Hu, X.; Beck, P.; Kiessling, L. L. *J. Am. Chem. Soc.* **1997**, *119*, 3161−3162.
(6) Zheng, M.; Manka, J. T.; Friedli, A. C. In *NASA Microgravity Materials Science Conference*; NASA Conf. Publ.: Huntsville, AL, 1998; pp 225−228.
(7) Douglass, A. G.; Zheng, M.; Friedli, A. C.; Kaszynski, P. *Polym. Prepr.* **1996**, *37*, 634.
(8) Gray, F. M. *Solid Polymer Electrolytes*; VCH: New York, 1991.

(9) Das, J.; Vu, T.; Harris, D. N.; Ogletree, M. L. *J. Med. Chem.* **1988**, *31*, 930−935.
(10) Cook, M. J.; Cracknell, S. J. *Tetrahedron* **1994**, *50*, 12125−12132.
(11) Bachrach, S. M. *J. Org. Chem.* **1995**, *60*, 4395−4398.
(12) Baggio, S.; Barriola, A.; de Perazzo, P. K. *J. Chem. Soc., Perkin Trans. 2* **1972**, 934−937.
(13) Calvo-Losada, S.; Suárez, D. *J. Am. Chem. Soc.* **2000**, *122*, 390−391.
(14) Dewar, M. J. S.; Pierini, A. B. *J. Am. Chem. Soc.* **1984**, *106*, 203−208.
(15) Lee, M. W.; Herndon, W. C. *J. Org. Chem.* **1978**, *43*, 518.
(16) Zhulin, V. M.; Bogdanov, V. S.; Kel'tseva, M. V.; Kabotyanskaya, E. B.; Koreshkov, Y. D. *Bull. Acad. Sci. Russ.* **1989**, *38*, 2303−2308.
(17) Zhulin, V. M.; Kel'tseva, M. V.; Bogdanov, V. S.; Koreshkov, Y. D.; Kabotyanskaya, E. B. *Bull. Acad. Sci. Russ.* **1990**, *39*, 456−459.
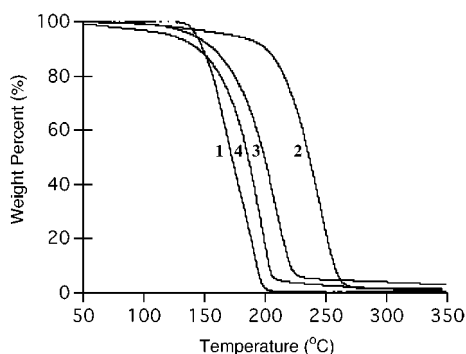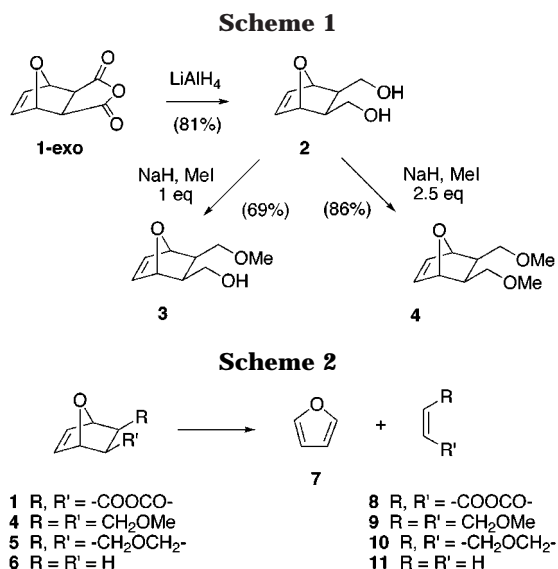
Scheme 1

Scheme 2

1 R, R' = -COOCO-
4 R = R' = CH₂OMe
5 R, R' = -CH₂OCH₂-
6 R = R' = H

8   R, R' = -COOCO-
9   R = R' = CH₂OMe
10 R, R' = -CH₂OCH₂-
11 R = R' = H

Figure 1. Thermal gravimetric analysis of compounds **1**−**4** heated at 20 °C/min under N₂.

product was reduced with lithium aluminum hydride to afford crude diol **2**. Williamson ether synthesis using carefully dried **2** and stoichiometric NaH in the presence of excess iodomethane produced monoether **3** in up to 69% yield. Product **3** was conveniently separated from byproducts **2** and **4** using an alumina column and a gradient of ethyl acetate and hexanes, which was effective even on a 0.1 mole scale. This represents a significant improvement over previous purification of small amounts of **3** using silica gel.[3] The double Williamson reaction of **2** with excess NaH followed by iodomethane resulted in an 86% yield of diether **4** after purification. A lower yield of **4** was obtained when higher temperatures were used during distillation.

Thermal Decomposition. Thermogravimetric Analysis (TGA) of **1**−**4** under a nitrogen atmosphere showed rapid and complete (>95%) weight losses between ∼200 and 260 °C (Figure 1). The lowest temperature for onset of decomposition was observed for **1** (147 °C) and highest for **2** (217 °C). The thermolysis of **4** gave two products which were identified by ¹H NMR analysis as furan (**7**) and *cis*-1,4-dimethoxy-2-butene (**9**), the expected products of the retro Diels−Alder reaction. (Scheme 2).

The kinetic behavior of the thermal decomposition of **4** was investigated at four temperatures using solution ¹H NMR spectroscopy. As the reaction proceeded, signals at 4.75 ppm in **4** disappeared while peaks consistent with **9**[19] appeared at 3.85 ppm in an otherwise uncomplicated
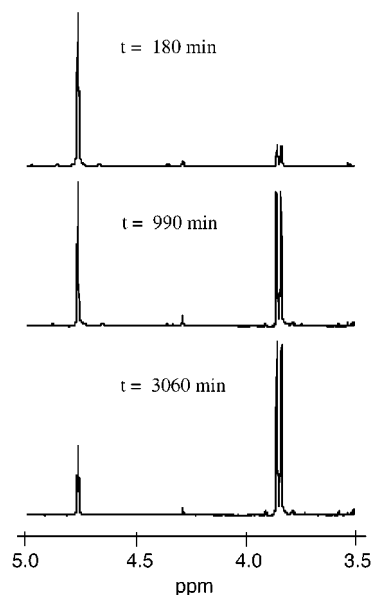
(18) Anet, F. A. L. *Tetrahedron Lett.* **1962**, *25*, 1219−1222.

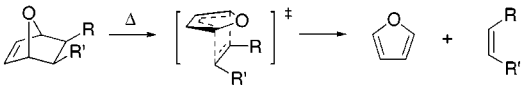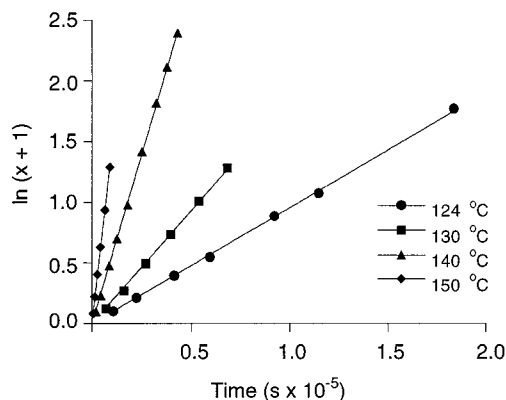**Figure 2.** ¹H NMR spectra showing progress of rDA reaction of **4** at 124 °C.

Figure 3. Plot of ln(*x* + 1) versus time for **4** at 124, 130, 140, and 150 °C, where *x* is the mole ratio of **4** to **9**. Rate constants were derived from the line slopes.

region of the spectrum (Figure 2). Integration of these peaks allowed the calculation of mole ratios of starting material and products. Application of the first-order kinetic formula $kt = \ln(x + 1)$, where *x* is the mole ratio of **4** to **9** present at a given time *t* and *k* is the rate constant, resulted in the plots shown in Figure 3. An Arrhenius plot of the kinetic data (included in the Supporting Information) allowed the calculation of activation energy E_a of 35.0 ± 0.5 kcal/mol and ln A = 1.77 (±0.03) × 10⁴ from the slope and intercept, respectively. The enthalpy and entropy of activation were calculated to be $\Delta H^{\ddagger}$ = 34.5 ± 0.5 kcal/mol and $\Delta S^{\ddagger}$ = 5.0 ± 0.1 cal/mol K. These values are higher than those measured for **1-exo**[14] by 9.5 kcal for $\Delta H^{\ddagger}$ and 4.8 cal/mol K for $\Delta S^{\ddagger}$ (Table 1).

Unfortunately, independent measurement of the thermodynamic values by differential scanning calorimetry (DSC) was difficult due to the superposition of several peaks. An endotherm (onset at 161 °C), presumably due to the vaporization of the rDA products **7** (bp 32 °C) and **9** (bp 141 °C), obscured the onset of the exotherm due to

(19) Malanga, C.; Mannucci, S.; Lardicci, L. *Tetrahedron* **1998**, *54*, 1021−1028.

Table 1. Calculated (B3LYP/6-31G*)[a] and Experimental[b] Thermochemical Parameters for the Retro Diels−Alder Reaction

compd	R, R'	reaction overall			activation parameters		
		ΔH	ΔS	ΔG	$\Delta H^{\ddagger}$	$\Delta S^{\ddagger}$	$\Delta G^{\ddagger}$
1-exo	-COOCO-	+3.44	+45.9	−10.2	22.4 (25.0)[c]	2.95 (0.17)[c]	21.6 (24.9)
5-anti	-CH$_2$OCH$_2$-	+3.07	+48.2	−11.3	31.8 (34.5)[d]	4.11 (5.0)[d]	30.5 (33.0)
6	H	+5.3 (−15.2)[e]	+43.5 (36.7)[e]	−7.6 (−6.7)[e]	31.2	3.1	30.3

[a] ΔG and ΔH are in units of kcal/mol; ΔS is in units of eu. The temperature for the gas-phase calculated values is 298 K. Full computational results are listed in the Supporting Information. [b] Experimental data is in parentheses. [c] Reference 14. [d] Diether **4**. [e] Reference 1.

the rDA reaction. The peak shape and position measured with DSC were highly dependent upon sample size and conditions. An example of a DSC thermogram of **4** appears in the Supporting Information.

Theoretical Analysis. The significant differences in the stability of the anhydride and the diether apparent from the TGA studies and measured activation energies for the rDA of **1** and **4** can be attributed[20] to the presence of conjugated carbonyl functionality in dienophile **8** as compared to an isolated alkene in **9**. To gain more insight into the electronic factors influencing these reactions, we sought to compare the calculated energies and transition state geometries.

The ground and transition state structures for anhydride **1-exo**, cyclic ether **5**, the parent 7-oxabicyclo[2.2.1]-hept-2-ene (**6**), and their respective rDA products: furan (**7**), maleic anhydride (**8**), 2,5-dihydrofuran (**10**), and ethylene (**11**), were calculated at the B3LYP/6-31G* level of theory using appropriate symmetry constraints. This level of theory has been successfully used in modeling concerted and stepwise pathways for the retro Diels−Alder and related pericyclic reactions,[21] as well as to explain the stereoselectivity of the DA reaction that produces **1-exo** as the major product.[13] The molecular geometries for the reagents, products, and transition states in the rDA reactions of the *exo* isomers of **1**, **5**, and **6** are shown in Figure 4. The calculated and experimental thermodynamic parameters for the rDA reactions are collected in Table 1.

The calculated structure for **1-exo** compares well to its experimental molecular geometry despite significant distortions in the solid-state environment (Figure 4). Most calculated bonds are longer than experimental but within one standard deviation of the X-ray data.[12] A notable exception is the C(2)−C(3) bond, which was calculated to be 0.06 Å shorter than the experimental result. The biggest disagreement in bond angles (up to 2°) involved the carbonyl groups. Ring puckering angles (Supporting Information) were found to be within 0.6° of the experimental values.

Activation parameters calculated for the rDA reaction of **1-exo** are close the experimental values[14] and similar to those calculated with perturbation methods.[13] The

(20) Fleming, I. A. *Pericyclic Reactions*; Oxford Science Publications: London, 1999.
(21) Tian, J.; Houk, K. N.; Klärner, F. G. *J. Phys. Chem.* **1998**, *102*, 7662−7667.

calculated $\Delta H^{\ddagger}_{298}$ is about 2.6 kcal/mol lower than the experimental value, while the $\Delta S^{\ddagger}$ is larger by 2.8 cal/mol K. The resulting $\Delta G^{\ddagger}$ of 3.3 kcal/mol reflects, to some degree, the difference between the environments used for calculations (gas-phase) and experiment (solution) in addition to systematic errors of the quantum-mechanical method.

Although the accurate quantitative reproduction of experimental values was not necessarily expected, the relative energies of the transition states should be modeled well because they are not affected much by solvent.[13,14] The effect of temperature upon the results was also expected to be small[21] so no attempt was made to correct to experimental temperature.

The tricyclic compound **5**, used as a model for dimethyl ether **4**, has two conformational minima corresponding to structures with oxygens on either the opposite (**5-anti**) or same (**5-syn**) side of the bicyclic ring. The former conformer is the global minimum on the potential energy surface (PES) and is separated from the less stable **5-syn** form ($\Delta G = 0.40$ kcal/mol) by an interconversion barrier of 2.1 kcal/mol. The transition state for the rDA reaction was identified as **5TS-syn**, and the analogous **5TS-anti** could not be located on the PES. The calculated thermodynamic parameters for **5TS-syn** differ from those measured experimentally for the diether **4** by about 2.5 kcal/mol, a coincidentally similar margin of error to that found for **1TS-exo**.

A comparison of the rDA reactions for the anhydride **1-exo** with its di-deoxy analogue **5** shows that both are entropically driven with almost identical overall thermodynamics. The small reaction endotherm (about 3 kcal/mol) is offset by a large entropy gain (about 46 cal/mol K) to give a moderate free energy gain of about −11 kcal/mol. The most significant difference between the two reactions is their TS energies. When compared to **1TS-exo**, the $\Delta G^{\ddagger}$ of **5TS** is higher by 8.9 kcal/mol, a value which is very close to the 8.1 kcal/mol difference between the experimental results (Table 1). The two PES's are graphically compared in Figure 5.

The calculated thermodynamic values for the rDA reaction of the parent 7-oxabicyclo[2.2.1]hept-2-ene (**6**) are similar to those for **5**, indicating that the perturbation of **6** by the oxymethyl substituents in **2**−**5** is small, almost negligible.

The observed difference in the TS energies between rDA reactions resulting in a conjugated dienophile (such as **8**) and the two with isolated double bonds (**10** and **11**) are reflected in the geometries of the TS state structures shown in Figure 4. The transition state **1TS-exo** is early relative to **5TS** (and **6TS**), with breaking C−C σ bonds at 2.117 Å, while in the latter, bond cleavage is further along, with C−C separations of about 2.158 Å (2.150 Å). The same trends are observed in the bond lengths of the furan ring and are consistent with an early transition state for the anhydride **1** decomposition.

These reactivity differences can be traced to the relative energies of the FMO's. For the forward DA reaction, the HOMO of furan (A$_2$, −6.11 eV) can be expected to interact with the same symmetry LUMO of the dienophile according to classical FMO theory.[20] According to our calculations, the LUMO (A$_2$, 0.50 eV) of the isolated C=C bond in dihydrofuran (**10**) is significantly higher in energy than that in maleic anhydride (**8**, A$_2$, −3.19 eV). This results in a 3.7 eV difference in the HOMO−LUMO gap for **7** and **8** relative to that
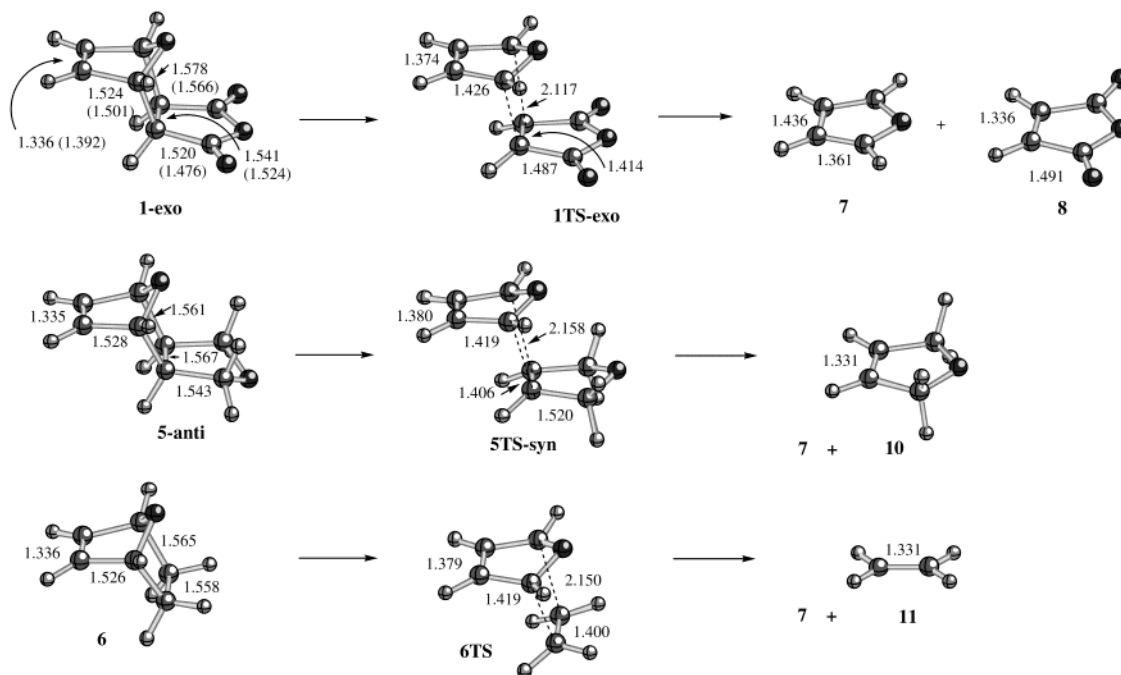
Figure 4. B3LYP/6-31G* geometries for **1-exo**, **5-anti**, and **6**, the transition states in the rDA reaction **1TS-exo**, **5TS-syn**, and **6TS**, and the respective products **7−11**. Bond lengths are in angstroms. Those in parentheses are experimental (ref 12).
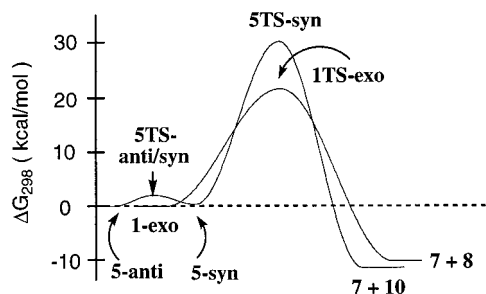

Figure 5. Reaction coordinate for the B3LYP/6-31G* Gibbs free energies calculated for **5**, **5TS**, and products **7** and **10** plotted with those for **1-exo**, **1TS-exo**, and products **7** and **8**.

between **7** and **10**. The better overlap between the FMOs in **7** and **8** lowers the energy of **1TS** by 9 kcal/mol below that of **5TS**.

The calculated activation parameters for the model rDA reactions of **5** and **6** were almost exactly the same: the two values of $\Delta H^{\ddagger}$ were within 0.5 kcal/mol of one another, and $\Delta S^{\ddagger}$ values were within 1.0 cal/mol K, resulting in $\Delta G^{\ddagger}$ values differing by only 0.2 kcal/mol. Compared to the experimental values for **4**, the calculated $\Delta G^{\ddagger}$ value for **5** was low by 2.5 kcal/mol (a difference of 2.7 kcal/mol for $\Delta H^{\ddagger}$ and 0.9 cal/mol K for $\Delta S^{\ddagger}$). These results affirm the validity of using **5**, a known compound,[22] as a model for **4**.[23] Furthermore, the influence of the methoxymethyl substitutents at the reaction center in **4** or **5** is minimal when compared to **6**.

Conclusions

The results for thermolysis of 7-oxabicyclo[2.2.1]-heptenes via the rDA reaction reported here are consis-

tent with expectations from qualitative FMO analysis. Diol **2** and related ethers **3** and **4** underwent the rDA reaction at relatively low temperatures, but higher than that required for the anhydride **1**. Kinetic data for the rDA reaction for **4** were closely comparable with calculated thermodynamic and kinetic parameters and experimental data on **1** from the literature. Generally, for the solution reactions described here, the kinetic and thermodynamic data compared unusually well quantitatively to the calculated (gas phase) data. Computational analysis of the transition states at the B3LYP/6-31G* level confirmed that the E_a in **1** is lowered by 9.5 kcal/mol relative to that of model compound **5**, a value almost identical to the difference in the experimental $\Delta H^{\ddagger}$ for **1-exo** and **4**. The faster rate of the rDA in **1** as compared to **4** is likely due to the energetic differences in the LUMO's of **8** and **9**.

Large entropic contributions to the rDA resulted in a favorable ΔG for the reactions of **1**, **5**, and **6**, overcoming a slightly unfavorable enthalpic term.

Experimental Section

Kinetics. Rates of retro Diels−Alder reactions were measured by following the decomposition of **4** by solution ^{1}H NMR. For each datapoint, a 20 μL sample was transferred with an Eppendorf pipet to an NMR tube and 0.6 mL of 1,2-dichlorobenzene-d_4 added. The solution was freeze−thaw degassed twice, and the NMR tube sealed under vacuum (∼50 Torr). Samples were immersed in a Fisher Isotemp 800 constant-temperature bath heated to 124 °C, 130 °C, 140 °C, or 150 °C ± 0.5 °C for at least six different time intervals corresponding to between 5 and 95% decomposition. Each decomposition was taken to at least three half-lives to determine whether the process was first order. The sample was periodically cooled to room temperature and the ratio of one product [^{1}H NMR δ 3.14−3.20 (m, max at 3.17, 6H), 3.84−3.87 (m, center at 3.85, 4H), 5.58−5.62 (m, max at 5.60, 2H)] to the starting material **4** [^{1}H NMR δ 1.73−1.80 (m, 2H), 3.07−3.2l (m, max at 3.17, 6H), 3.22−3.35 (m, 2H), 4.72−4.75 (m, max at 4.75, 4H), 6.13 (m, max at 6.13, 2H)] was monitored by ^{1}H NMR (200 MHz).

(22) Gilchrist, T. L.; Wood, J. E. *J. Chem. Soc., Perkin Trans. 1* **1992**, 9−15.
(23) The relatively high calculated stability of **5** and its similarity to **1** and **4** is inconsistent with the identification of **5** as an unstable structure.

The assignment of structures of the products was confirmed by comparison to a published ^{1}H NMR spectrum of **9**[19] and NMR of pure **7** in 1,2-dichlorobenzene-d_4 [^{1}H NMR δ 6.22 (t, $J = 1.3$ Hz, 2H), 7.27 (t, $J = 1.2$ Hz, 2H)]. The enthalpies and entropies of activation were calculated using standard formulas: $\Delta H^\ddagger = -E_a - RT$ and $\Delta S^\ddagger = R[\ln A - \ln(ekT/h)]$.

Computational Methods. Quantum-mechanical calculations were carried out using the Gaussian 98 package[24] on an SGI PowerIndigo2 workstation, and the resulting energies are listed in the Supporting Information. Geometry optimizations were undertaken using appropriate symmetry constraints at the B3LYP/6-31G* level of theory.[25] Transition states were located using the QTS2 procedure. Vibrational frequencies were used to characterize the nature of the stationary points and to obtain thermodynamic parameters. Zero-point energy corrections (ZPEC) were calculated using a 0.9804 scaling factor.[26] Thermodynamic properties were calculated at 298 K and 1 atm.

Synthesis. Boiling and melting points are uncorrected. ^{1}H NMR and ^{13}C NMR spectra were run at 200 and 50 MHz, respectively. Samples were dissolved in deuteriochloroform and referenced to CHCl$_3$ unless noted otherwise. IR spectra were measured as neat samples. Commercial reagents were used as received. Tetrahydrofuran were dried over benzophenone ketyl and distilled before use. Differential scanning calorimetry measurements were run on a Perkin-Elmer DSC-7 under nitrogen calibrated to an indium standard. Aluminum pans (50 μL) with a pinhole and sample sizes of 2−5 mg were used and the heating rate was 20 °C/min. Thermal gravimetric analysis measurements were done using a Perkin-Elmer TGA-7 under nitrogen. Samples with weights ranging from 15 to 20 mg were heated from 40 to 350 °C at a rate of 20 °C/min. Compound **1**[27] was synthesized according to a modification of the method of Furdík[28] (for details see Supporting Information).

***exo,exo*-7-Oxabicyclo[2.2.1]hept-5-ene-2,3-dimethanol (2).**[9] Following a modification of the method of Novak,[29] a dry 2 L three-necked round-bottomed flask equipped with a pressure equalizing dropping funnel and reflux condenser was charged with LiAlH$_4$ (17.1 g, 0.45 mol) and THF (125 mL). Anhydride **1** (60.0 g, 0.361 mol) was dissolved in warm THF (850 mL) and added dropwise to the stirred slurry. The mixture was allowed to stir overnight, and then water (20 mL), NaOH (20 mL, 15% w/w), and water (55 mL) were then added slowly in sequence. The resulting white suspension was filtered through Celite and rinsed with THF (50 mL). The solvent was removed by rotary evaporation and residue was dried in vacuo and over P$_2$O$_5$ to give 48.1 g (81.0%) of a colorless, opaque, viscous oil of pure *exo, exo* isomer: ^{1}H NMR δ 1.84−1.95 (m, max at 1.89, 2H), 3.52−3.76 (m, max at 3.66, 4H), 4.51 (bs, 2H), 4.63 (s, 2H), 6.32 (s, 2H).

Extraction of the filtered solids using a Soxhlet apparatus for 48 h with methylene chloride gave a mixture of isomers (3.8 g) in a 3:2 ratio. Overlapping NMR signals ascribed to *exo, exo* at δ 1.84−1.95 (m, max at 1.89, 2H) were comparable to literature values[9] δ 1.92 (m, 2H) and signals ascribed to the *endo, endo* isomer at δ 1.77−1.84 (m, max at 1.80, 2H) appeared in the same region of the spectrum (see Supporting Information).

***exo*-2-Hydroxymethyl-*exo*-3-methoxymethyl-7-oxabicyclo[2.2.1]hept-5-ene (3).**[3] The reaction was done on 0.1 mol to 5 mmol scales according to literature procedure.[3] Good quality NaH (1.1 equiv, 60% in oil) was introduced into a dry round-bottomed flask and THF (1 mL/mmol NaH) was added to form a slurry. The reaction vessel was cooled to 0 °C and **2** (1.0 equiv), dissolved in THF (1 mL/mmol **2**), was added dropwise. The mixture was stirred for 30 min at 0 °C, and then methyl iodide (1.1 eq) added dropwise. The mixture was stirred for 30 min and then allowed to warm to room temperature and stir for 3 h. The mixture was filtered through Celite, the solid washed with THF (0.5 mL/mmol **3**), and the solvent removed. The product was purified by column chromatography on neutral alumina (80−200 mesh) packed in hexanes using 1:4 ethyl acetate/hexanes eluent, gradually changing the gradient to 4:1 ethyl acetate:hexanes as products eluted. The chromography was followed using 1:1 ethyl acetate: hexanes R_f (**2**) ∼ 0; R_f (**3**) ∼ 0.5; R_f (**4**) ∼1. A single column could be loaded heavily and used repeatedly without hindering separation. After separation and solvent removal, **3** was obtained as a pale yellow oil, but yield varied from 35 to 69%. ^{1}H NMR δ 1.83−2.04 (m, max at 1.97, 2H), 3.26 (bs, 1H), 3.26−3.78 (m, 4H), 3.35 (s, 3H), 4.66 (m, 1H), 4.70 (m, 1H), 6.32−6.39 (m, center at 6.38, 2H); ^{13}C NMR δ 40.2, 42.9, 59.1, 62.7, 73.3, 81.2, 81.5, 135.7, 136.3.

***exo,exo*-5,6-Dimethoxymethyl-7-oxabicyclo[2.2.1]hept-2-ene (4).**[29] Sodium hydride (10.0 g, 60% in oil, 0.25 mol) was weighed into a dry 500 mL round-bottomed flask in a glovebag and covered with dry THF (125 mL). Diol **2** (15.6 g, 0.100 mol) in THF (50 mL) was added dropwise via addition funnel, and the mixture was stirred for 1 h. Methyl iodide (31.8 g, 0.22 mol) was added through the rinsed funnel. After 1 h, wet ether was added until no bubbling was noted. The solution was dried over magnesium sulfate and filtered, the solvent was removed, and the crude product was Kugelrohr distilled to give 15.9 g (86.1%) of pale yellow oil: bp (lit.[29] 60−65 °C, 0.001 Torr, 75−80 °C (0.5 Torr); ^{1}H NMR δ 1.62−1.68 (m, max at 1.65, 2H), 2.98−3.26 (m, max at 3.09, 4H), 3.11 (s, 6H), 4.57 (t, $J = 0.8$ Hz, 2H), 6.09 (t, $J = 0.9$ Hz, 2H).

Supporting Information Available: Tables of computed energies for structures discussed in the text, calculated rates, and puckering angles, a DSC thermogram, NMR spectra relevant to the thermal decomposition of **4**, an ^{1}H NMR spectrum of the **2** *exo* and *endo* isomer mixture, an Arrhenius plot, and some experimental descriptions are included. This material is available free of charge via the Internet at http:/pubs.acs.org.

JO0003091

(24) Frisch, M. J.; Trucks, G. W.; Schlegel, H. B.; Scuseria, G. E.; Robb, M. A.; Cheeseman, J. R.; Zakrzewski, V. G.; J. A. Montgomery, J.; Stratmann, R. E.; Burant, J. C.; Dapprich, S.; Millam, J. M.; Daniels, A. D.; Kudin, K. N.; Strain, M. C.; Farkas, O.; Tomasi, J.; Barone, V.; Cossi, M.; Cammi, R.; Mennucci, B.; Pomelli, C.; C. Adamo; Clifford, S.; Ochterski, J.; Petersson, G. A.; Ayala, P. Y.; Cui, Q.; Morokuma, K.; Malick, D. K.; Rabuck, A. D.; Raghavachari, K.; Foresman, J. B.; Cioslowski, J.; Ortiz, J. V.; Baboul, A. G.; Stefanov, B. B.; Liu, G.; Liashenko, A.; Piskorz, P.; Komaromi, I.; Gomperts, R.; Martin, R. L.; Fox, D. J.; Keith, T.; Al-Laham, M. A.; Peng, C. Y.; Nanayakkara, A.; Gonzalez, C.; Challacombe, M.; Gill, P. M. W.; Johnson, B.; Chen, W.; Wong, M. W.; Andres, J. L.; Gonzalez, C.; Head-Gordon, M.; Replogle, E. S.; Pople, J. A. In Gaussian, Inc.: Pittsburgh, PA, 1998.
(25) Becke, A. D. *J. Chem. Phys.* **1993**, *98*, 5648−5652.
(26) Scott, A. P.; Radom, L. *J. Phys. Chem.* **1996**, *100*, 16502−16513.
(27) Diels, O.; Alder, K. *Chem. Ber.* **1929**, *62*, 554−558.
(28) Furdík, M.; Drábek, J. *Acta Fac. Rerum Nat. Univ. Comenianae, Chim.* **1965**, 23−24.
(29) Novak, B. M. Ph.D. Thesis, California Institute of Technology, 1989.